

# Polystyrene Nanoplastics Trigger Changes in Cell Surface Properties of Freshwater and Marine Cyanobacteria

Nigarsan Kokilathanan<sup>1</sup>, Basirath Raof<sup>1</sup>, and Maria Dittrich<sup>1,2\*</sup>

<sup>1</sup>Biogeochemistry Group, Department of Physical and Environmental Sciences, University of Toronto Scarborough, 1065 Military Trail, Toronto, ON, M1C 1A4, Canada

<sup>2</sup>Department of Earth Sciences, University of Toronto St. George, 22 Ursula Franklin Street, Toronto, ON, M5S 3B1, Canada

\*Corresponding author: Maria Dittrich, m.dittrich@utoronto.ca

## 1. Supplementary Information

### 1.1. Cyanobacteria Cell Cultures

**ASN-III** consists of 25.0 g L<sup>-1</sup> NaCl, 3.5 g L<sup>-1</sup> MgSO<sub>4</sub>·7H<sub>2</sub>O, 2.0 g L<sup>-1</sup> MgCl<sub>2</sub>·6H<sub>2</sub>O, 0.75 g L<sup>-1</sup> NaNO<sub>3</sub>, 0.75 g L<sup>-1</sup> K<sub>2</sub>HPO<sub>4</sub>·3H<sub>2</sub>O, 0.50 g L<sup>-1</sup> CaCl<sub>2</sub>·2H<sub>2</sub>O, 0.50 g L<sup>-1</sup> KCl, 0.02 g L<sup>-1</sup> NaCO<sub>3</sub>, 3.0 mg L<sup>-1</sup> Citric acid, 3.0 mg L<sup>-1</sup> Fe-ammonium citrate, 500.0 µg L<sup>-1</sup> Mg-EDTA, 10.0 µg L<sup>-1</sup> Vitamin B<sub>12</sub>, 2.86 mg L<sup>-1</sup> H<sub>3</sub>BO<sub>3</sub>, 1.81 mg L<sup>-1</sup> MnCl<sub>2</sub>·4H<sub>2</sub>O, 22.0 µg L<sup>-1</sup> ZnSO<sub>4</sub>·7H<sub>2</sub>O, 390.0 µg L<sup>-1</sup> NaMoO<sub>4</sub>·2H<sub>2</sub>O, 79.0 µg L<sup>-1</sup> CuSO<sub>4</sub>·5H<sub>2</sub>O, and 49.4 µg L<sup>-1</sup> Co(NO<sub>3</sub>)<sub>2</sub>·6H<sub>2</sub>O. The pH of the growth medium was adjusted to 7.4 ± 0.03 using 1 M HCl under sterile conditions<sup>1</sup>. The zeta potential of the ASN-III medium was 5.53 ± 0.83 mV.

**Zarrouk Medium** consists of 16.8 g L<sup>-1</sup> NaHCO<sub>3</sub>, 0.5 g L<sup>-1</sup> K<sub>2</sub>HPO<sub>4</sub>, 2.5 g L<sup>-1</sup> NaNO<sub>3</sub>, 1.0 g L<sup>-1</sup> NaCl, 1.0 g L<sup>-1</sup> K<sub>2</sub>SO<sub>4</sub>, 0.2 g L<sup>-1</sup> MgSO<sub>4</sub>·7H<sub>2</sub>O, 0.2 g L<sup>-1</sup> CaCl<sub>2</sub>·2H<sub>2</sub>O, 0.01 g L<sup>-1</sup> FeSO<sub>4</sub>·7H<sub>2</sub>O, 0.08 g L<sup>-1</sup> EDTA, 2.86 mg L<sup>-1</sup> H<sub>3</sub>BO<sub>3</sub>, 1.81 mg L<sup>-1</sup> MnCl<sub>2</sub>·4H<sub>2</sub>O, 22 µg L<sup>-1</sup> ZnSO<sub>4</sub>·7H<sub>2</sub>O, 390 µg L<sup>-1</sup> Na<sub>2</sub>MoO<sub>4</sub>·2H<sub>2</sub>O, and 80 µg L<sup>-1</sup> CuSO<sub>4</sub>·5H<sub>2</sub>O. The pH of the medium was 8.0 ± 0.2<sup>2</sup>. The zeta potential of the Zarrouk medium was -12.73 ± 0.40 mV.

## 1.2. Cell Count Calibration Curves

Cell cultures were diluted and washed twice with Milli-Q water before filtering through black 0.2  $\mu\text{m}$  Nucleopore polycarbonate (PC) filters. Cell enumerations were performed at a magnification of 1000x for *Syn. PCC8806* and 100x for *Spirulina* with 10 random microscope fields using the cellSens® imaging system of an Olympus IX 51 microscope with TRITC filter (543/22 nm Excitation, 593/40 nm Emission). Total cell count (cells  $\text{L}^{-1}$ ) was determined using calibration curves of absorbance (OD650 and OD680) against cell enumerations<sup>1</sup> (**Fig. S1**).

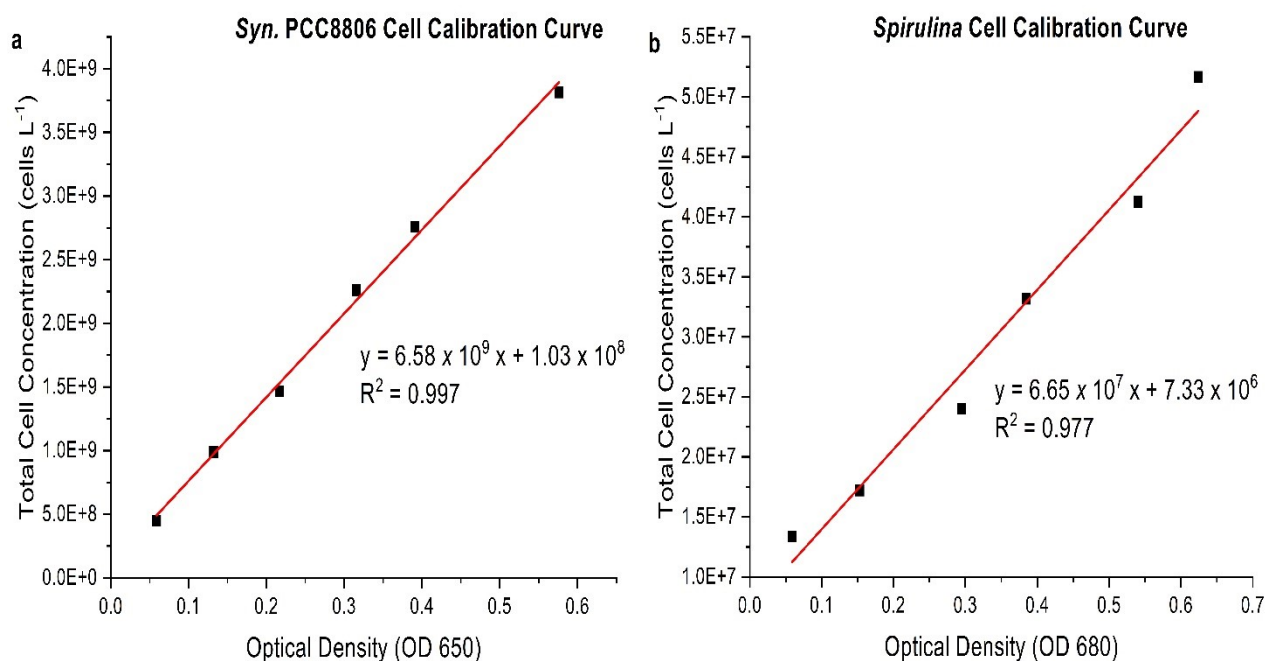


**Fig. S1. Cell count calibration curves.** Cell enumerations (cells  $\text{L}^{-1}$ ) against optical density readings (OD 650 and OD 680) for **a.** PCC8806 and **b.** *Spirulina*.

## 1.3. Particle Number Concentration (PNC) and Particle Size Distribution

The number of particles in a solution can be determined by the particle number concentration (PNC). PNC is calculated based on the following equation:

$$\text{PNC} = \frac{\text{Mass Concentration}}{\text{Mass per Nanoparticle}} = \frac{3 \times \text{Mass Concentration}}{4\pi \times r^3 \times \rho} \quad (\text{particles L}^{-1})$$

Where the density of PS ( $\rho$ ) =  $1.05 \text{ g} \cdot \text{cm}^3 = 1050 \text{ mg} \cdot \text{cm}^3$ , and  $r$  is the average radius of the nanoparticle ( $274.75 \text{ nm} = 2.7475 \times 10^{-5} \text{ cm}$ ); mass concentrations are 2, 10, or 20  $\text{mg L}^{-1}$ .

PNCs for 2, 10, and 20  $\text{mg L}^{-1}$  are  $2.2 \times 10^{10}$  particles  $\text{L}^{-1}$ ,  $1.1 \times 10^{11}$  particles  $\text{L}^{-1}$  and  $2.2 \times 10^{11}$  particles  $\text{L}^{-1}$ , respectively.

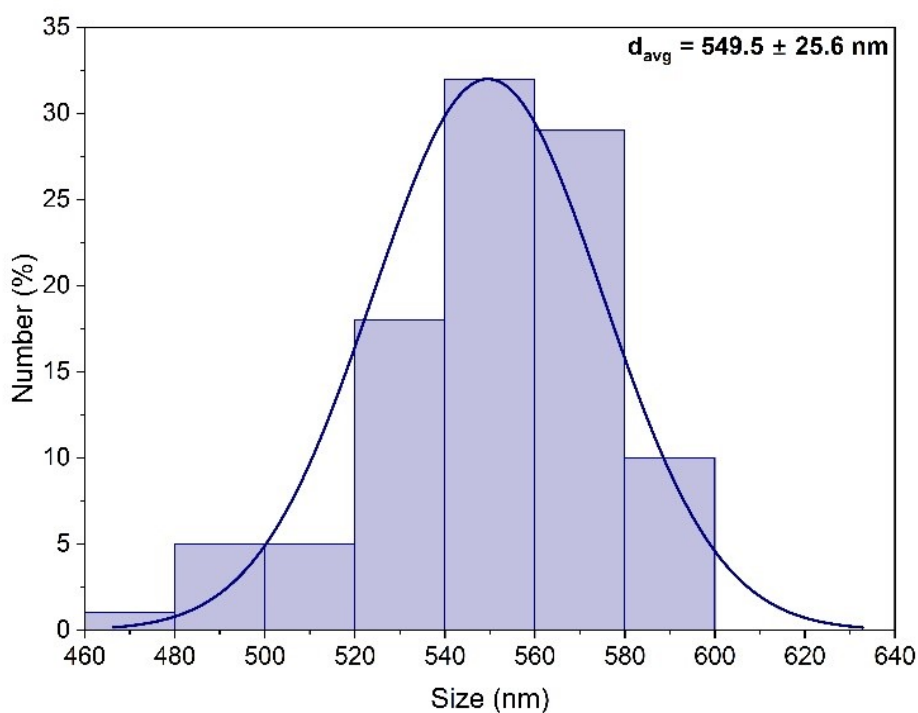


**Fig. S2. Particle Size Distribution of PS NPLs.** The size distribution of PS NPLs is based on TEM images ( $n = 100$ ).

#### 1.4. Zeta Potential of PS NPIs

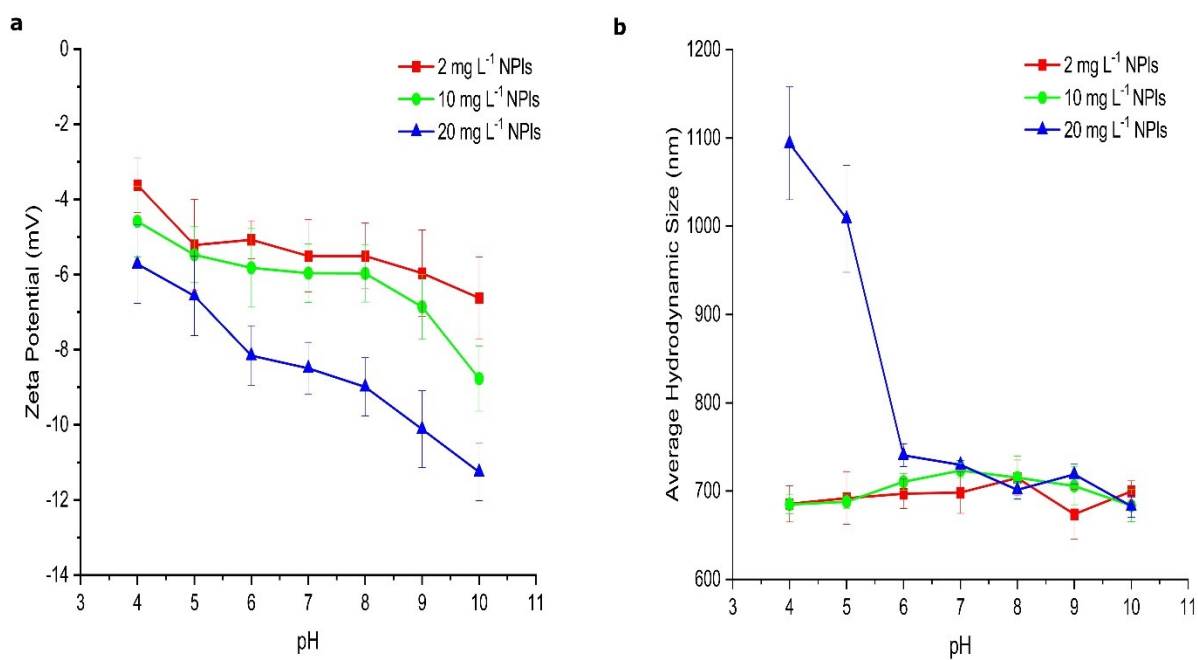


**Fig. S3. Measurements of PS NPIs under a constant electrolyte. Average a. ZPs and b. HDs** of the three PS NPIs concentrations in 0.1 M NaNO<sub>3</sub> at pH 4 to 10. Values are shown as mean  $\pm$  SD,  $n = 9$ .

### 1.5. TEM Images and Cell Wall Thickness

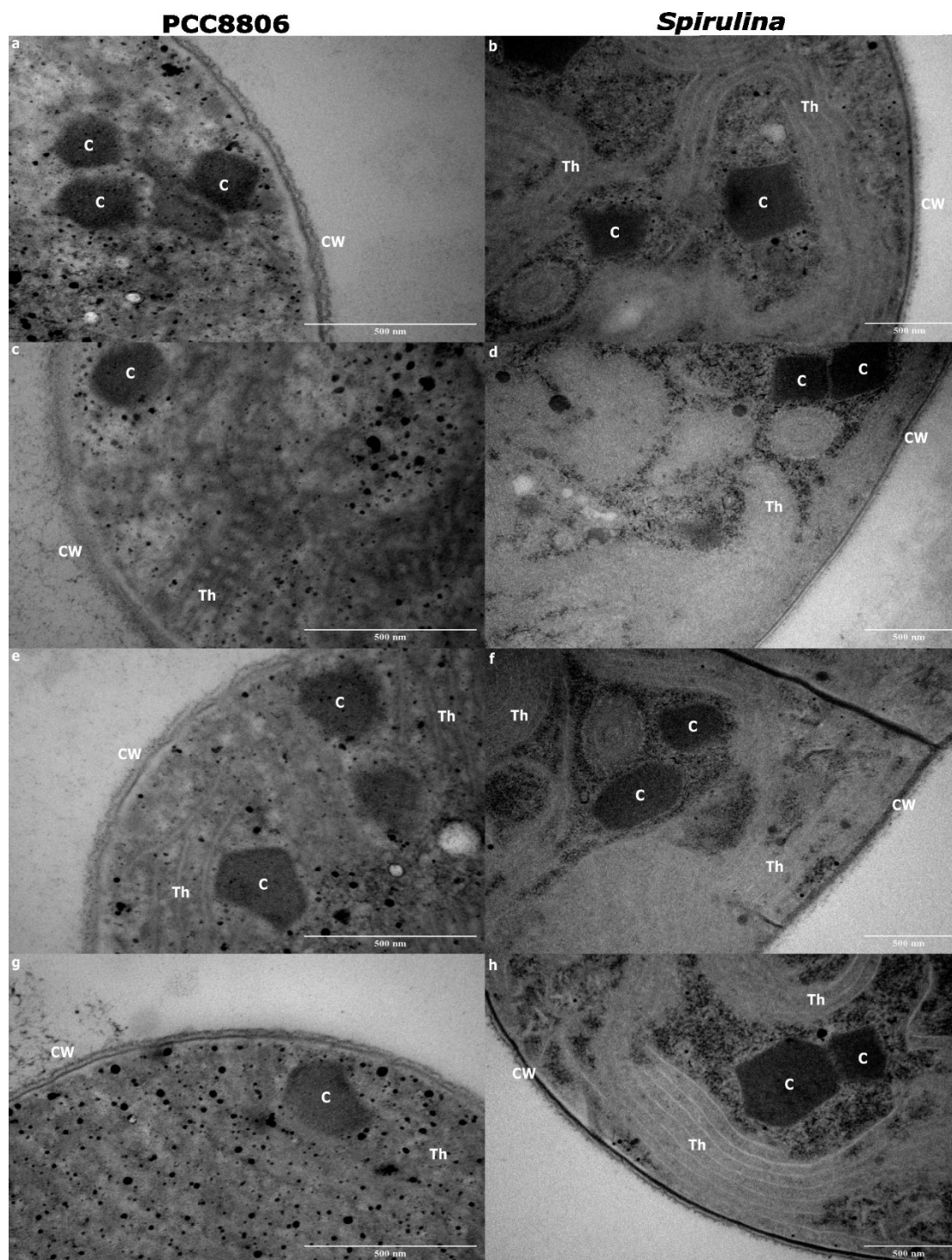


**Fig. S4. Ultrastructure of PCC8806 and *Spirulina* exposed to PS NPLs.** TEM images of PCC8806 and *Spirulina* cells at the exponential phase: **a, b.** Control, **c, d.** exposed to 2 mg L<sup>-1</sup>

PS NPIs, **e, f.** exposed to 10 mg L<sup>-1</sup> PS NPIs, **g, h.** exposed to 20 mg L<sup>-1</sup> PS NPIs. **C** – carboxysomes, **Th** – thylakoid membranes, **CW** – cell wall<sup>3</sup>.

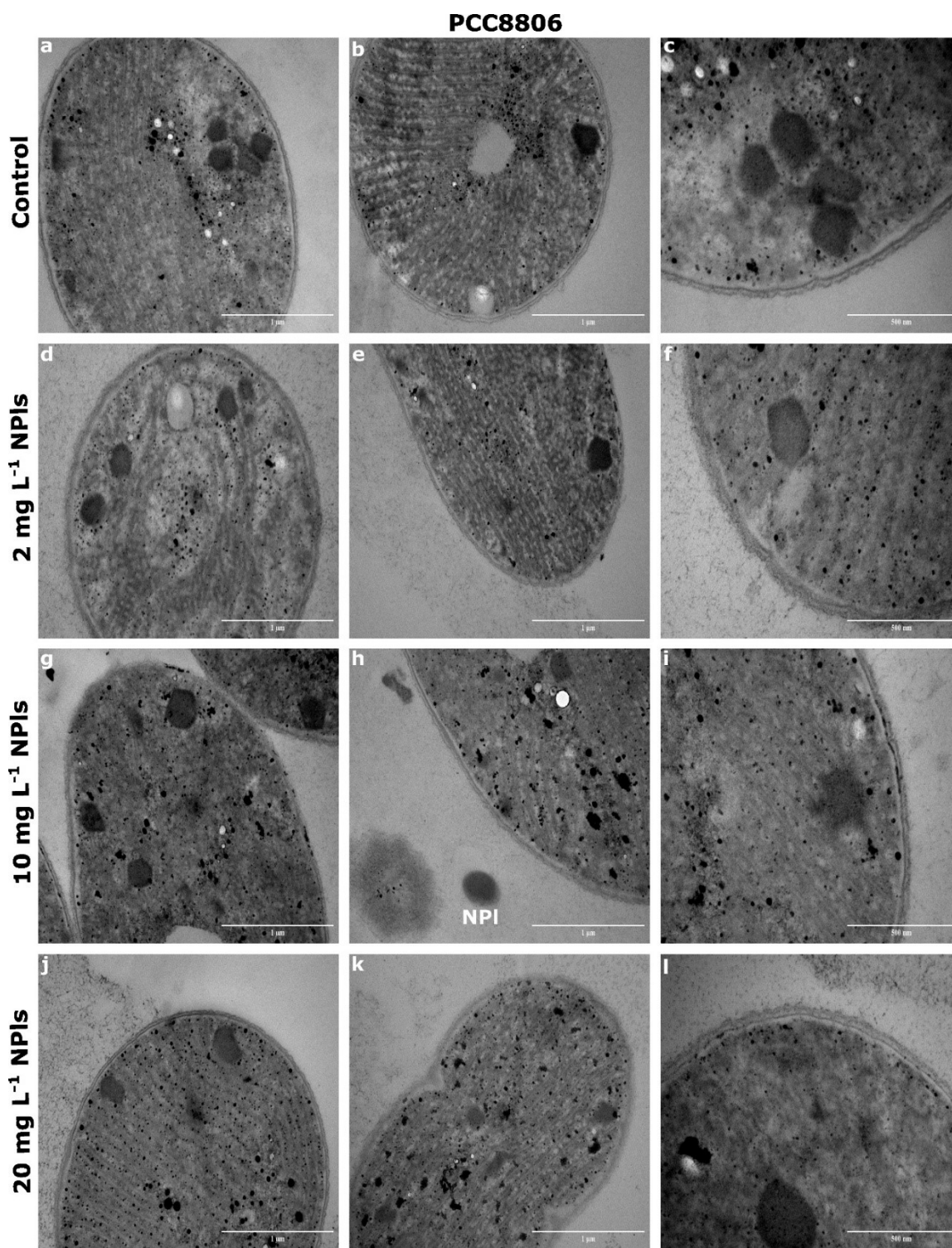


**Fig. S5. Ultrastructure of PCC8806 exposed to PS NPIs at various magnifications. TEM** images of PCC8806 at the exponential phase: **a-c.** Control, **d-f.** exposed to 2 mg L<sup>-1</sup> PS NPIs, **g-i.** exposed to 10 mg L<sup>-1</sup> PS NPIs, **j-l.** exposed to 20 mg L<sup>-1</sup> PS NPIs. A PS NPI was observed adjacent to, but not interacting with, the cell surface of PCC8806.

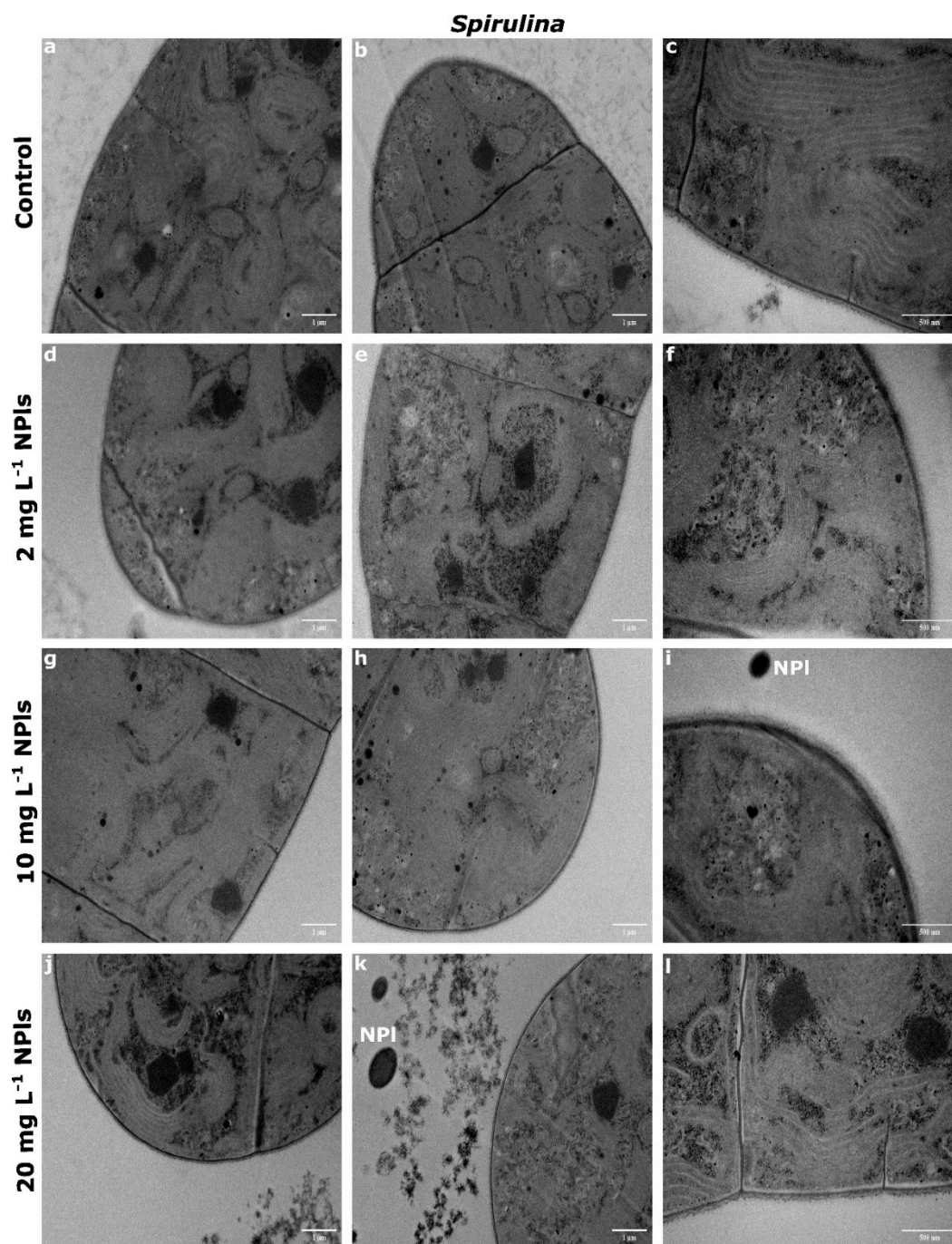


**Fig. S6. Ultrastructure of *Spirulina* exposed to PS NPs at various magnifications.** TEM images of *Spirulina* at the exponential phase: **a-c.** Control, **d-f.** exposed to 2 mg L<sup>-1</sup> PS NPs, **g-i.** exposed to 10 mg L<sup>-1</sup> PS NPs, **j-l.** exposed to 20 mg L<sup>-1</sup> PS NPs. A few PS NPs were observed adjacent to the cell surfaces of *Spirulina*, with stained organic matter.

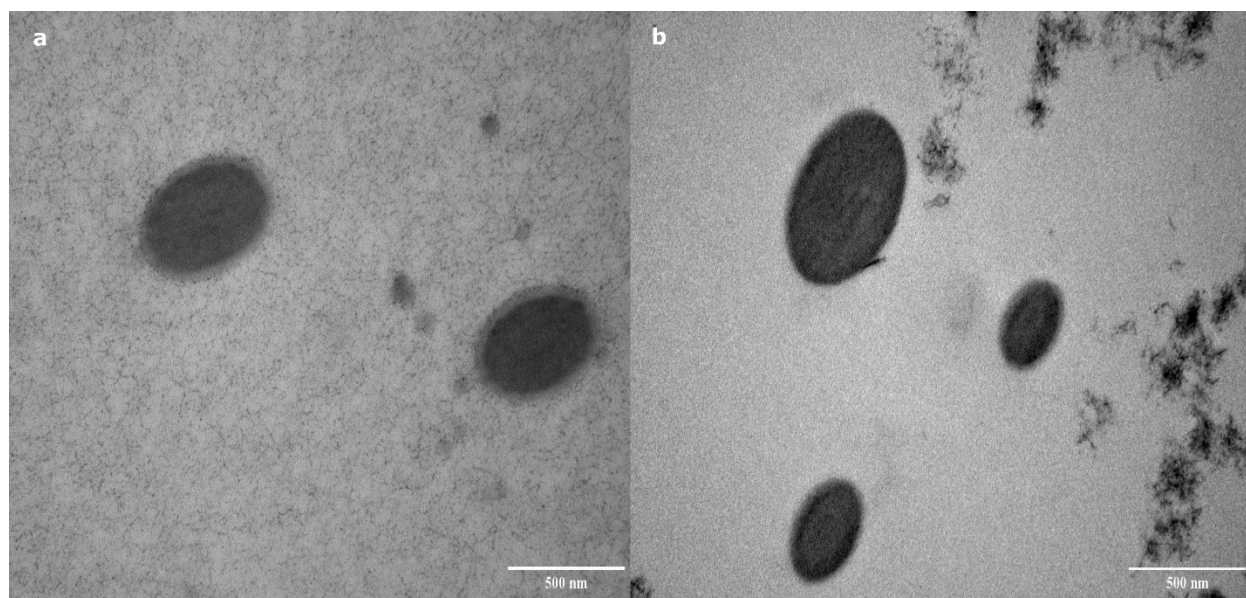


**Fig. S7. TEM images of PS NPs.** TEM images of **a.** PS NPs after undergoing the same sample preparation. **b.** PS NPs were observed adjacent to the cell surfaces of *Spirulina* exposed to 20 mg L<sup>-1</sup> PS NPs.

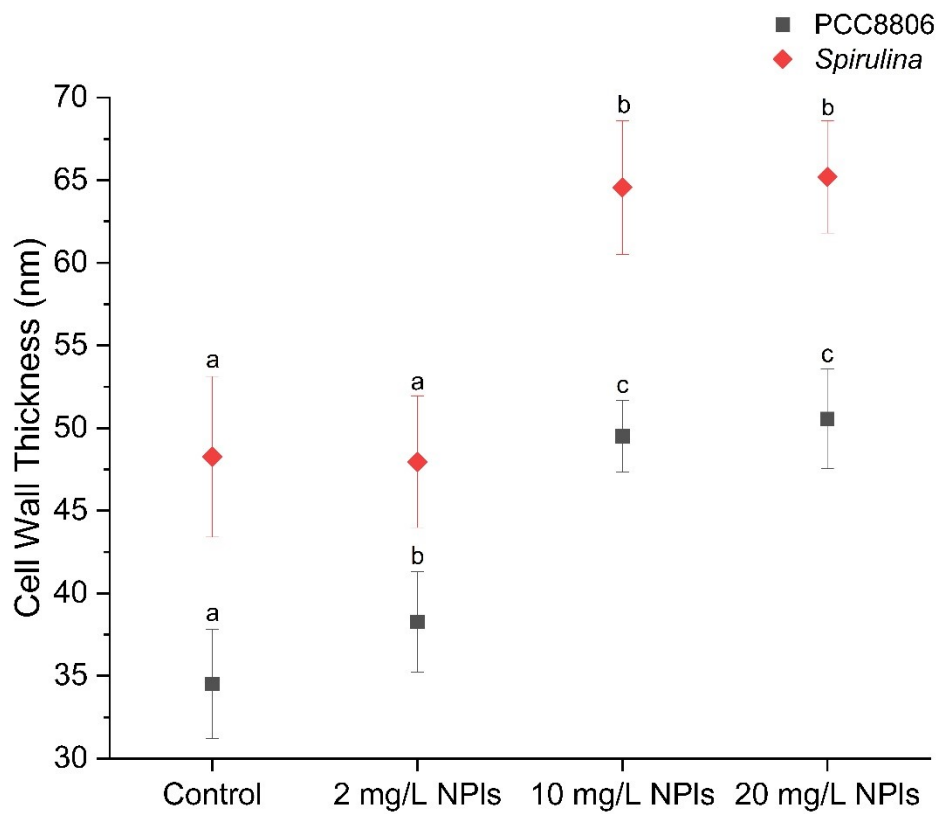


**Fig. S8.** Cell wall thickness of PCC8806 and *Spirulina* cells. Values are shown as mean  $\pm$  STD,  $n = 15$ . Different letters indicate significant differences between treatments ( $p < 0.05$ ) within each cyanobacterial species.

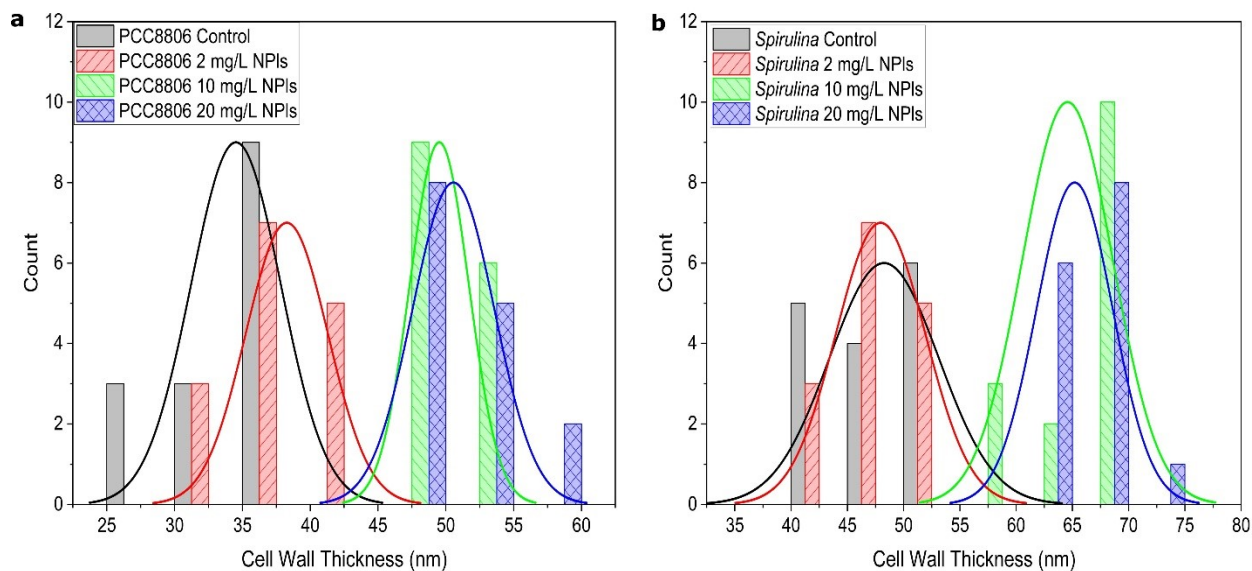


**Fig. S9.** Distribution of cell wall thickness of PCC8806 and *Spirulina* cells ( $n = 15$ ).

**Table S1.** Raw cell wall thickness measurements of PCC8806 and *Spirulina*. Values are shown as mean  $\pm$  STD,  $n = 15$ . Different letters indicate significant differences between treatments ( $p < 0.05$ ) within each cyanobacterial species.

Cell Wall Thickness (nm)	PCC8806	<i>Spirulina</i>
Control	34.52 $\pm$ 3.32 <sup>a</sup>	48.26 $\pm$ 4.86 <sup>a</sup>
2 mg L <sup>-1</sup>	38.27 $\pm$ 3.03 <sup>b</sup>	47.95 $\pm$ 3.97 <sup>a</sup>
10 mg L <sup>-1</sup>	49.51 $\pm$ 2.18 <sup>c</sup>	64.57 $\pm$ 4.04 <sup>b</sup>
20 mg L <sup>-1</sup>	50.56 $\pm$ 3.02 <sup>c</sup>	65.19 $\pm$ 3.39 <sup>b</sup>

### 1.6. ATR-FTIR Spectra and Tables

**Table S2.** Assignments of peaks found on the PCC8806 ATR-FTIR spectra<sup>4, 5</sup>.

Wavenumber (cm <sup>-1</sup> )				Peak Assignments
PCC8806				
Control	2 mg L <sup>-1</sup> NPIs	10 mg L <sup>-1</sup> NPIs	20 mg L <sup>-1</sup> NPIs	
669, 701	663, 706	663, 699	669, 699	C-H out-of-plane bending vibrations and C-H of aromatic

				rings
763	763	763	763	Out-of-plane bending vibrations
855	854	854	855	$\nu$ N-H wag from the presence of primary and secondary amines
955	954	927, 954	955	$\nu_s, \nu_{as}$ P-OH and P-O-P of phosphate groups in phosphate oligomers; May contain contributions from glycosidic linkage
994, 1044	995, 1037	995, 1021, 1044	994, 1044	$\nu$ C-O and C-C of pyranose
1079	1078	1078	1077	$\nu_s$ P=O of general phosphoryl groups present in the phosphodiester backbone of nucleic acid (DNA and RNA); May contain contributions from the presence of phosphorylated proteins and polyphosphate
1152	1152	1152	1152	$\nu$ C-O of C-O-C glycosidic bridges in polysaccharides
1244	1243	1243	1244	$\nu_{as}$ P=O of general phosphoryl groups present in the phosphodiester backbone of nucleic acid (DNA and RNA) or polyphosphate
1340	1335	1342	1340	$\nu$ C-O of carboxylic acid or esters
1399	1403	1399	1399	$\delta$ CH <sub>2</sub> and $\delta$ CH <sub>3</sub> and $\nu_s, \delta$ C-OH of carboxylic groups (COO <sup>-</sup> )
1453	1452	1452	1453	$\delta$ CH <sub>2</sub> and $\delta$ CH <sub>3</sub> of proteins; CH <sub>3</sub> scissoring (amide III band)
1536	1536	1536	1536	$\delta$ N-H, $\nu$ C-N, and $\nu$ C=O of amides in proteins (amide II band)
1656	1657	1657	1656	$\nu$ C=O of amides in proteins; (amide I band)
1739	1740	1768	1739	$\nu$ C=O of protonated carboxylic acid groups (COOH) and of ester functional groups in lipids

$\delta$  = bending,  $\nu$  = stretching,  $\nu_{as}$  = asymmetric stretching,  $\nu_s$  = symmetric stretching

**Table S3.** Assignments of peaks found on the *Spirulina* ATR-FTIR spectra<sup>4-6</sup>.

Wavenumber (cm <sup>-1</sup> )				Peak Assignments
<i>Spirulina</i>				
Control	2 mg L <sup>-1</sup> NPIs	10 mg L <sup>-1</sup> NPIs	20 mg L <sup>-1</sup> NPIs	
619, 701, 721	619, 701, 719	619, 701, 719	619, 701, 719	C-H out-of-plane bending vibrations and C-H of aromatic rings
741	742	742	741	Out-of-plane bending vibrations
882	883	883	846, 883	vN-H wag from the presence of primary and secondary amines
921, 979	923, 983	924, 984	924, 985	v <sub>s</sub> , v <sub>as</sub> P-OH and P-O-P of phosphate groups in phosphate oligomers; May contain contributions from glycosidic linkage
1042	1045	1045	1029	vC-O and C-C of pyranose
1154	1158	1158	1155	vC-O of C-O-C glycosidic bridges in polysaccharides
1262	1259	1259	1261	v <sub>as</sub> P=O of general phosphoryl groups present in the phosphodiester backbone of nucleic acid (DNA and RNA) or polyphosphate
1342	1340	1324	1324	vC-O of carboxylic acid or esters
1402	1399	1414, 1427	1413, 1427	δCH <sub>2</sub> and δCH <sub>3</sub> and v <sub>s</sub> , δC-OH of carboxylic groups (COO <sup>-</sup> )
1440, 1501	1441, 1502	1502	1501	δCH <sub>2</sub> and δCH <sub>3</sub> of proteins; CH <sub>3</sub> scissoring (amide III band)
1537	1538	1538	1557	δN-H, C-N stretching, and vC=O of amides in proteins (amide II band); May also contain contributions from vC=N
1655	1657	1657	1661	vC=O of amides in proteins (amide I band)
1771	1773	1773	1776	vC=O of protonated carboxylic acid groups (COOH) and of ester functional groups in lipids

δ = bending, v = stretching, v<sub>as</sub> = asymmetric stretching, v<sub>s</sub> = symmetric stretching

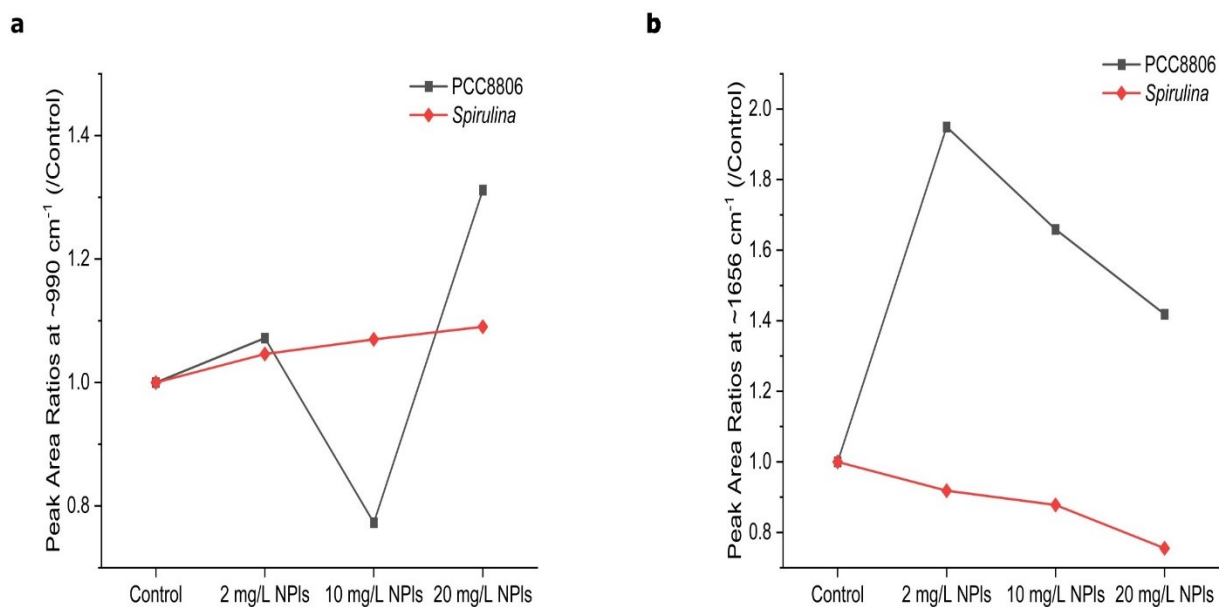


**Fig. S10. Peak Area Ratio of Polysaccharides and Proteins under the Presence of PS NPIs.**

Ratios of the peak area of PCC8806 and *Spirulina* at **a.**  $\sim 990\text{ cm}^{-1}$  and **b.**  $\sim 1656\text{ cm}^{-1}$  under PS NPI exposure compared to the peak area of the control. Peak areas were determined using deconvolution analysis. The peak at  $\sim 990\text{ cm}^{-1}$  represents polysaccharides, whereas the peak at  $\sim 1656\text{ cm}^{-1}$  represents proteins.

**Table S4.** FTIR deconvolution analysis of PCC8806 peaks at  $\sim 990\text{ cm}^{-1}$  (polysaccharides) and  $\sim 1656\text{ cm}^{-1}$  (proteins).

PCC8806	Peak Center (cm <sup>-1</sup> )	Area Fit	Adjusted R <sup>2</sup> Value
Control	995.6	121.0	0.939
	1656.3	62.1	
2 mg L <sup>-1</sup>	993.4	129.7	0.969
	1655.9	121.1	

10 mg L <sup>-1</sup>	996.1	93.5	0.979
	1656.4	103.1	
20 mg L <sup>-1</sup>	993.9	158.7	0.919
	1652.6	88.1	

**Table S5.** FTIR deconvolution of *Spirulina* peaks at ~990 cm<sup>-1</sup> (polysaccharides) and ~1656 cm<sup>-1</sup> (proteins).

<i>Spirulina</i>	Peak Center (cm <sup>-1</sup> )	Area Fit	Adjusted R <sup>2</sup> Value
Control	977.2	3.2	0.986
	1657.1	92.3	
2 mg L <sup>-1</sup>	977.4	3.3	0.994
	1656.5	84.7	
10 mg L <sup>-1</sup>	978.0	3.4	0.992
	1657.9	81.0	
20 mg L <sup>-1</sup>	978.3	3.5	0.989
	1660.9	69.6	

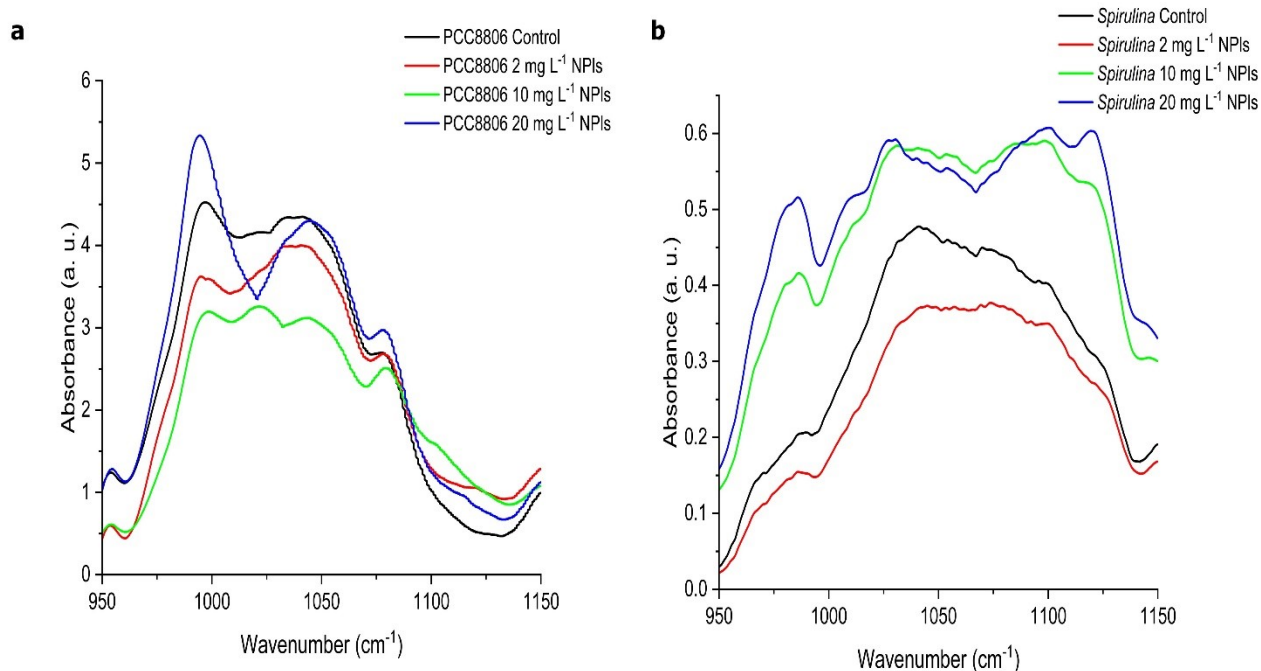


**Fig. S11. Zoomed-in ATR-FTIR Spectra.** ATR-FTIR Spectra of **a.** PCC8806 and **b.** *Spirulina* at 950-1150  $\text{cm}^{-1}$ .

The penetration depth ( $d_p$ ) of ATR-FTIR can be calculated from the following equation<sup>4</sup>:

$$d_p = \frac{\lambda}{2\pi[n_c^2 \times \sin^2 \theta - n_s^2]^{1/2}}$$

Where  $\theta$  is the angle of incidence,  $\lambda$  is the wavelength of the beam ( $\text{cm}^{-1}$ ), and  $n_s$  and  $n_c$  are the refractive indices of the sample and ATR crystal, respectively. For a diamond crystal (refractive index = 2.4) with an incident angle of  $45^\circ$ , and assuming the refractive index of bacterial cells is approximately 1.39,  $d_p$  is around  $0.908 \mu\text{m}$  at  $1800 \text{ cm}^{-1}$  and about  $2.725 \mu\text{m}$  at  $600 \text{ cm}^{-1}$ .

### 1.7. XPS Spectra and Table

From the initial survey XPS spectra (**Fig. S7**), the high-resolution spectra of carbon, nitrogen, and oxygen peaks were linked and convoluted to specific functional groups (**Figs. S8 and S9**), and molar ratios relative to total carbon were estimated to define their relative proportion (**Tables 2 and 3**).

The carbon peak was deconvolved into four components, with the most significant peak for PCC8806 and *Spirulina* found at the binding energy of  $\sim 248.8$  eV (C1s), assigned to carbon bound only to carbon and hydrogen, commonly associated with lipids or amino acids. The other carbon components detected include at  $\sim 286.0$  eV (C1s A), assigned to carbon singly bound to oxygen or nitrogen, which includes ether, alcohol, amine, and amide groups; at  $\sim 287.5$  eV (C1s B), assigned to a double-bonded carbon with oxygen (C=O) or two single-bonded oxygen with carbon (O-C-O), including carbonyl, carboxyl, amide, acetyl, and hemiacetal groups<sup>7, 8</sup>; and at  $\sim 288.5$  eV (C1s C), associated with carbon forming one double bond and a single bond with oxygen (O-C=O), which corresponds to carboxyl or ester groups.

The oxygen peak was deconvolved into three components: A peak at  $\sim 530.7$  eV (O1s) assigned to oxygen forming a double bond with carbon (O=C), a double bond with phosphorus (O=P), or oxygen forming a single bond with phosphate (P-O-Ring) in esters, amides, and phosphate groups; a peak at  $\sim 531.7$  eV (O1s A) attributed to hydroxide groups, acetal, and hemiacetal; and a peak at  $\sim 532.7$  eV (O1s B) corresponded to oxygen forming a single bond with hydrogen (HO-C), such as hydroxyl groups or carbon (C-O-C), such as acetal and hemiacetals<sup>7, 9</sup>.

The nitrogen peak was deconvolved into two components: A peak at  $\sim 399.5$  eV (N1s) is attributed to unprotonated amine or amide functional groups, whereas a peak at  $\sim 400.5$  eV (N1s A) is assigned to protonated amine or amide functional groups.

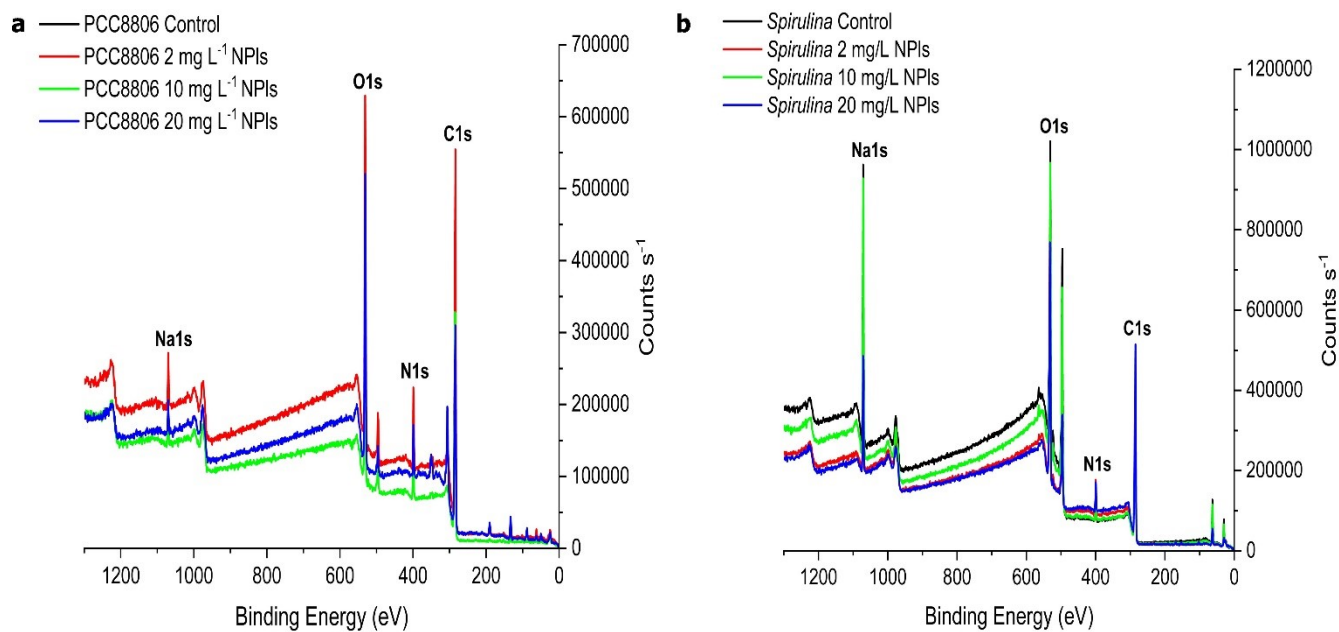


**Fig. S12. Low-resolution XPS Spectra.** Survey XPS spectra of **a.** PCC8806 and **b.** *Spirulina* at the exponential phase under control and NPI-exposed conditions. The Na1s peak was attributed to the washing procedure of the cells.

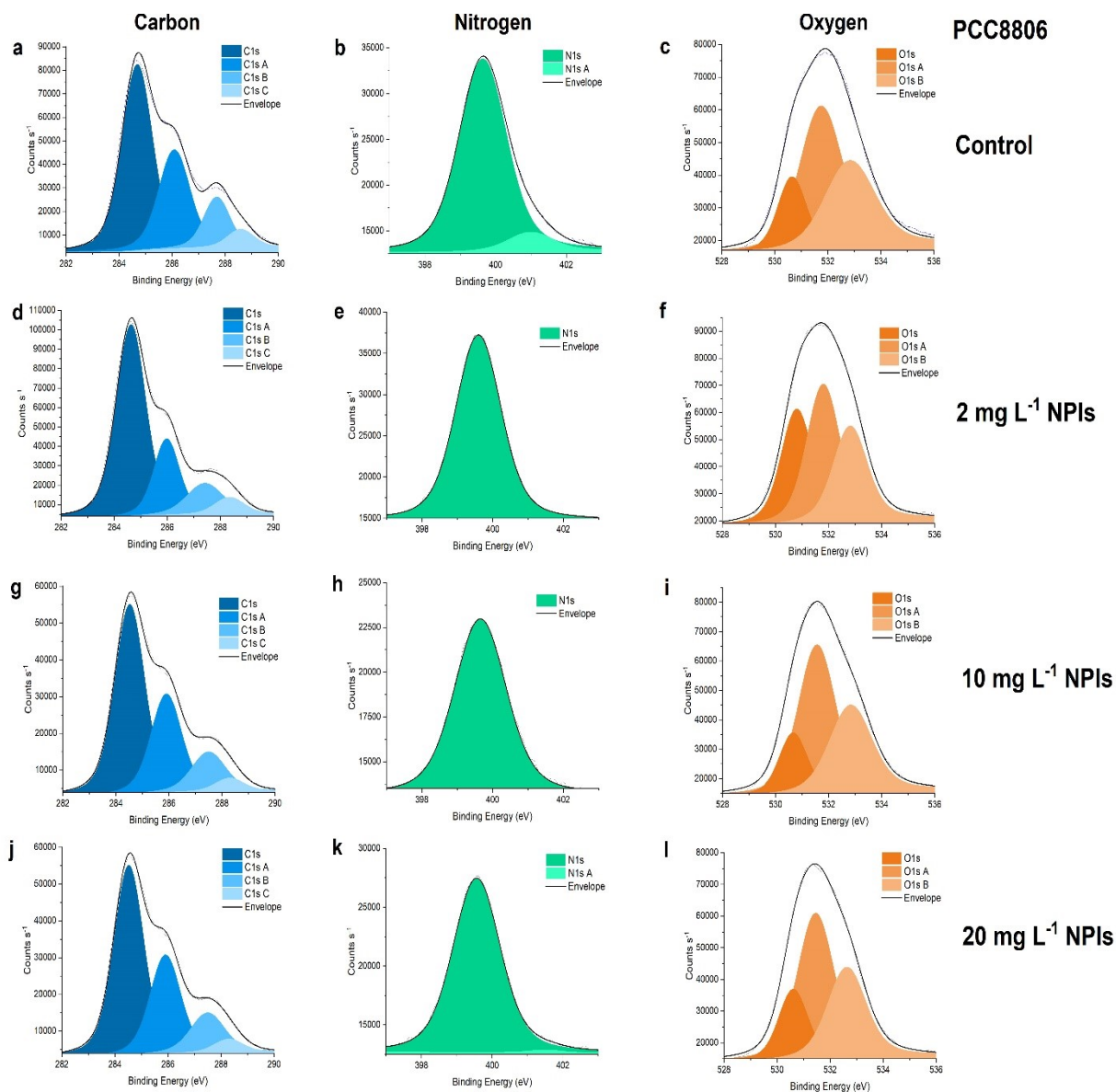


**Fig. S13. High-resolution XPS Spectra of PCC8806.** High-resolution XPS spectra of carbon (C1s), nitrogen (N1s), and oxygen (O1s) of PCC8806. **a-c.** Control, **d-f.** with 2 mg L<sup>-1</sup> PS NPIs, **g-i.** with 10 mg L<sup>-1</sup> PS NPIs, **j-l.** with 20 mg L<sup>-1</sup> PS NPIs.

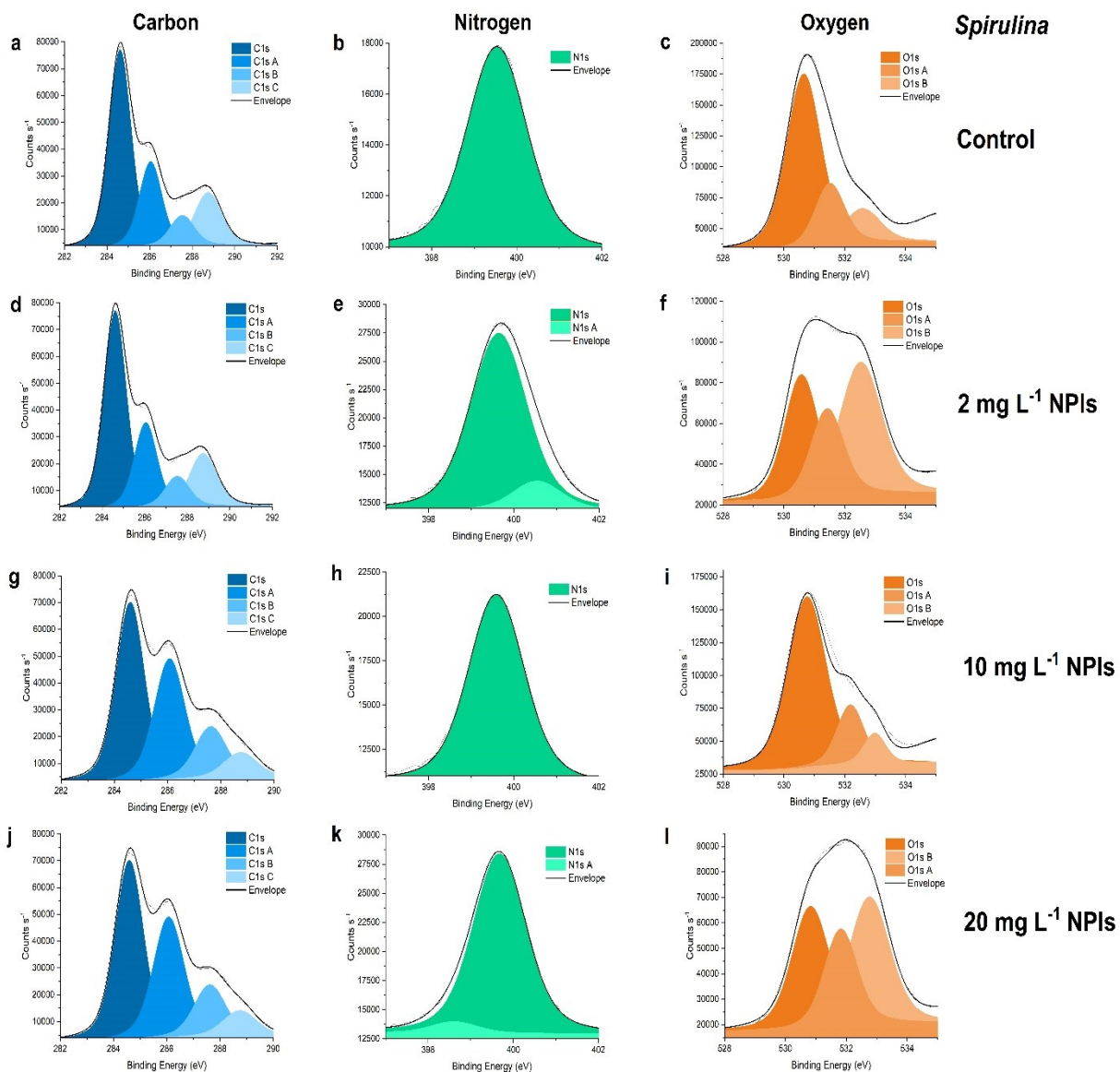


**Fig. S14. High-resolution XPS Spectra of *Spirulina*.** High-resolution XPS spectra of carbon (C1s), nitrogen (N1s), and oxygen (O1s) of *Spirulina*. **a-c.** Control, **d-f.** with 2 mg L<sup>-1</sup> PS NPIs, **g-i.** with 10 mg L<sup>-1</sup> PS NPIs, **j-l.** with 20 mg L<sup>-1</sup> PS NPIs.

**Table S6.** Raw XPS data of PCC8806 at the exponential phase. FWHM – Full Width at Half Maximum.

	Name	Peak Energy	FWHM	Area	Atomic
--	------	-------------	------	------	--------

		eV	eV	P (CPS.eV)	(%)
<b>PCC8806 Control</b>	C1s	284.68	1.37	126727.42	36.66
	N1s	399.64	1.6	39316.67	7.33
	O1s	531.74	1.9	96621.22	11.56
	C1s A	286.08	1.4	69060.17	19.99
	C1s B	287.68	1.18	29732.74	8.62
	C1s C	288.58	1.2	10752.69	3.12
	O1s A	530.64	1.27	33711.13	4.03
	O1s B	532.83	2.23	67095.81	8.04
	N1s A	400.99	1.49	3511.66	0.66
<b>PCC8806 2 mg L<sup>-1</sup></b>	C1s	284.63	1.34	154776.31	41.83
	N1s	399.59	1.53	40134.17	6.99
	O1s	531.80	1.49	88499.04	9.90
	C1s A	285.98	1.16	53508.59	14.47
	C1s B	287.42	1.64	30883.30	8.36
	C1s C	288.34	1.34	13661.53	3.70
	O1s A	530.80	1.42	70291.43	7.85
	O1s B	532.82	1.53	61614.45	6.89
<b>PCC8806 10 mg L<sup>-1</sup></b>	C1s	284.69	1.49	62964.16	30.09
	N1s	399.65	1.76	19994.51	6.16
	O1s	531.56	1.67	98642.46	19.50
	C1s A	286.08	1.44	35096.38	16.79
	C1s B	287.68	1.08	11995.70	5.74
	C1s C	288.48	1.16	5678.85	2.72
	O1s A	530.66	1.27	31252.06	6.17
	O1s B	532.83	1.9	64828.98	12.83
<b>PCC8806 20 mg L<sup>-1</sup></b>	C1s	284.52	1.35	81841.55	33.79
	N1s	399.56	1.60	27578.13	7.34
	O1s	531.45	1.64	87880.90	15.01
	C1s A	285.90	1.38	43498.70	17.98

	C1s B	287.49	1.53	19418.79	8.03
	C1s C	288.29	1.31	5524.87	2.29
	O1s A	530.60	1.31	34191.36	9.64
	O1s B	532.63	1.71	56409.25	5.84
	N1s A	401.51	1.14	303.85	0.08

**Table S7.** Raw XPS data of *Spirulina* at the exponential phase. FWHM – Full Width at Half Maximum.

	Name	Peak Energy eV	FWHM eV	Area P (CPS.eV)	Atomic (%)
<b><i>Spirulina</i> Control</b>	C1s	284.61	1.3	99353.00	29.24
	N1s	399.53	1.69	15546.76	2.95
	O1s	530.65	1.37	224686.67	27.34
	C1s A	285.97	1.32	34072.36	10.04
	C1s B	287.61	1.63	18327.09	5.4
	C1s C	288.88	1.45	38125.64	11.25
	O1s A	531.52	1.16	67328.48	8.2
	O1s B	532.59	1.42	45816.58	5.58
<b><i>Spirulina</i> 2 mg L<sup>-1</sup></b>	C1s	284.59	1.27	99692.10	27.45
	N1s	399.65	1.59	28647.34	5.08
	O1s	531.43	1.31	67098.62	7.64
	C1s A	286.07	1.38	72983.46	20.12
	C1s B	287.62	1.42	32030.99	8.84
	C1s C	288.74	1.51	16761.26	4.63
	O1s A	530.58	1.34	96805.73	11.02
	O1s B	532.53	1.66	127158.71	14.49
	N1s A	400.54	1.39	4130.51	0.73
<b><i>Spirulina</i> 10 mg L<sup>-1</sup></b>	C1s	284.62	1.24	107751.41	30.86
	N1s	399.59	1.58	19441.22	3.59

	OIs	530.76	1.50	228477.55	27.05
	CIs A	286.05	1.27	47195.89	13.53
	CIs B	287.53	1.38	18535.91	5.32
	CIs C	288.75	1.53	35532.02	10.20
	OIs A	532.18	1.06	56292.92	6.67
	OIs B	532.98	0.86	23295.93	2.76
<b><i>Spirulina</i></b> <b>20 mg L<sup>-1</sup></b>	CIs	284.60	1.2	127462.72	34.77
	NIs	399.67	1.5	26771.54	4.71
	OIs	531.82	1.31	58943.86	6.65
	CIs A	285.82	1.09	47151.56	12.87
	CIs B	286.48	0.89	21333.34	5.83
	CIs C	287.95	1.97	54400.28	14.87
	OIs A	530.82	1.48	83387.85	9.40
	OIs B	532.76	1.60	94188.36	10.64
	NIs A	398.61	1.31	1497.49	0.26

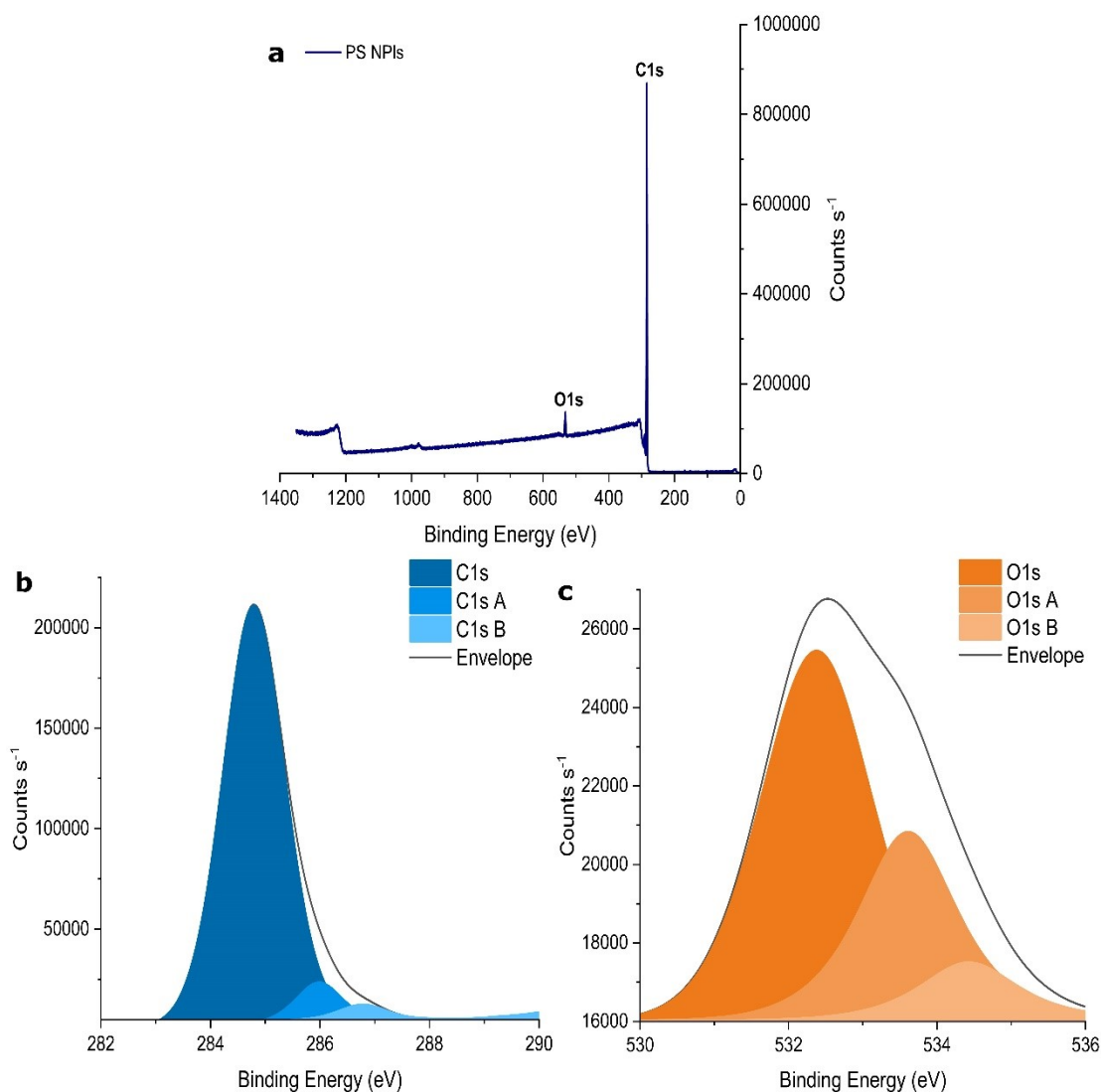


**Fig. S15. XPS Survey and High-Resolution Spectra of PS NPIs. a.** Survey XPS spectrum and High-resolution XPS spectra of **b.** Carbon (C1s) and **c.** Oxygen (O1s) of PS NPIs.

**Table S8.** Raw XPS data of PS NPIs. FWHM – Full Width at Half Maximum.

Name	Peak Energy eV	FWHM eV	Area P (CPS.eV)	Atomic (%)
C1s	284.79	1.33	299309.26	88.64
O1s	532.38	1.77	18164.02	2.23
C1s A	285.98	0.94	18722.32	5.55

C1s B	286.78	0.98	7539.79	2.24
O1s A	533.61	1.54	8523.81	1.05
O1s B	534.43	1.51	2488.98	0.31

**Table S9.** Binding Energies (eV), mass fractions (%), and high-resolution XPS spectral band assignments of PS NPIs<sup>7, 10</sup>.

<b>Element/Ratio</b>	<b>Peak Energy eV</b>	<b>PS NPIs Mass Fraction (%)</b>	<b>Assignment</b>
Total C	284.29	96.4	
Total O	532.18	3.6	
O/C		0.0	
C1s	284.79 ± 0.51	91.9	C-(C, H)
C1s A	285.98	5.8	C-O
C1s B	286.78	2.3	C=O; O-C-O
O1s	532.13 ± 0.35	62.1	O=C
O1s A	533.37 ± 0.35	29.2	C-OH; C-O-C
O1s B	534.19 ± 0.35	8.6	HO-C

## 1.8. EPS Determination and Visualization

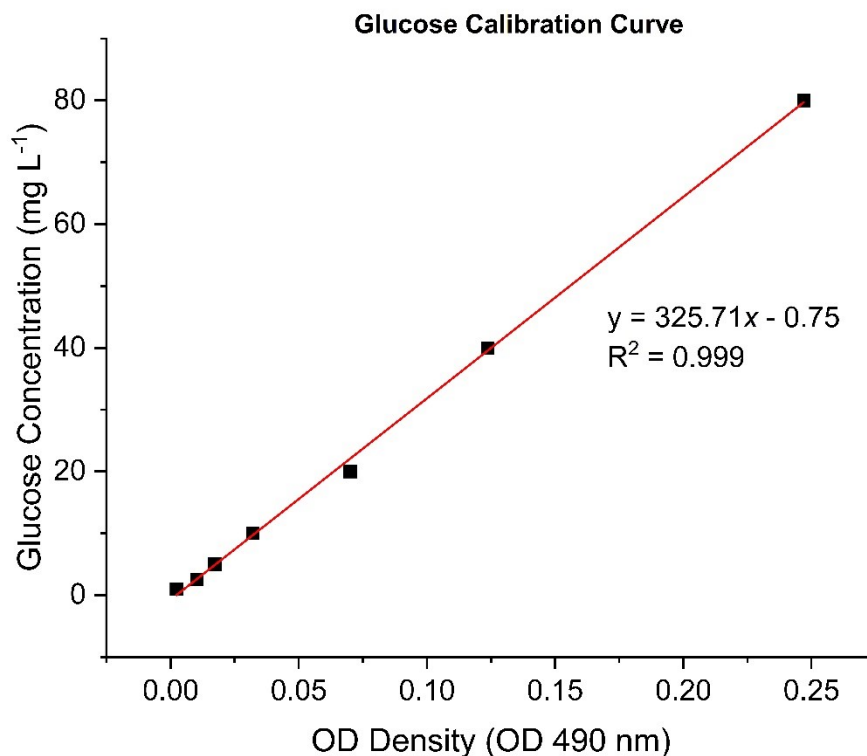


**Fig. S16. Glucose standard calibration curves.** Glucose concentrations ( $\text{mg L}^{-1}$ ) against optical density readings at 490 nm (OD 490).

**Table S10.** Raw EPS concentrations of PCC8806 and *Spirulina* under NPI exposure. Values are shown as mean  $\pm$  SD,  $n = 9$ . Different letters indicate significant differences between treatments ( $p < 0.05$ ).

NPI Concentration ( $\text{mg L}^{-1}$ )	EPS Concentration ( $\text{mg L}^{-1}$ )	
	PCC8806	<i>Spirulina</i>
Control	$4.79 \pm 0.88^a$	$5.44 \pm 1.33^a$
2	$7.50 \pm 2.46^{ab}$	$11.99 \pm 4.63^b$
10	$8.99 \pm 3.65^b$	$18.40 \pm 4.37^c$
20	$9.27 \pm 2.73^b$	$25.49 \pm 4.36^d$

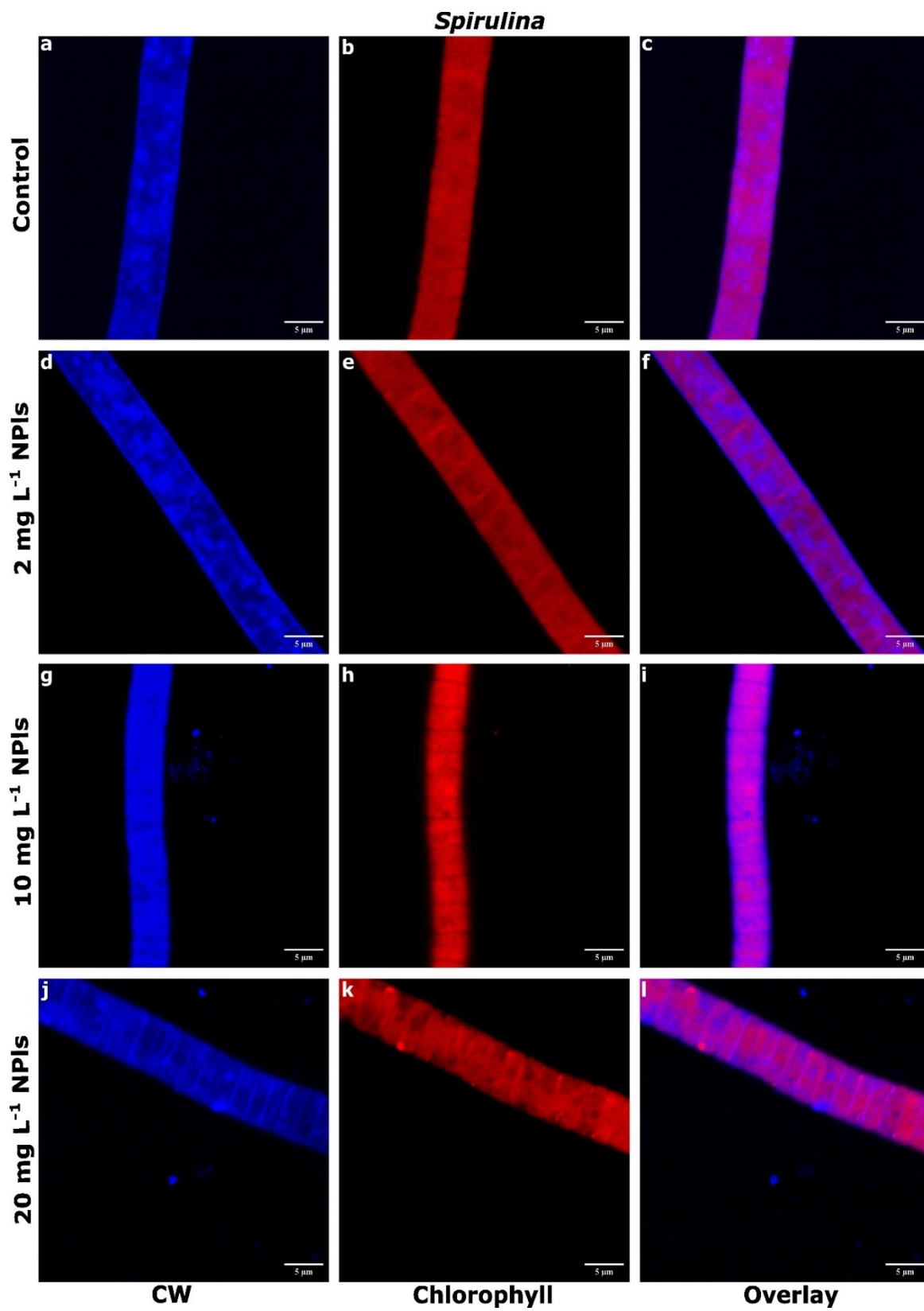


**Fig. S17. EPS Secretion of *Spirulina* under NPI Exposure.** LSCM images of *Spirulina* cells at the exponential phase. **a-c.** Control, **d-f.** with 2 mg L<sup>-1</sup> PS NPIs, **g-i.** with 10 mg L<sup>-1</sup> PS NPIs, **j-l.** with 20 mg L<sup>-1</sup> PS NPIs. The scale bar is 5 μm. Cells were stained with calcofluor white (CW) for polysaccharides. Images (**c, f, i, l**) represent the overlay of CW staining and chlorophyll fluorescence. A purple color indicates a higher presence of polysaccharides.

### 1.9. Stokes' Law

The sedimentation rate of NPI aggregates can be estimated using Stokes' law. Stokes' velocity ( $V_s$ ) is calculated from the following equation:

$$V_s = \frac{d^2 \times g \times (\rho_p - \rho_m)}{18 \times \mu}$$

Where  $d$  = hydrodynamic diameter of the NPI aggregates in the medium, the density of PS ( $\rho_p$ ) = 1.05 g · cm<sup>3</sup> = 1050 kg · m<sup>3</sup>, the density of the medium ( $\rho_m$ ) = 1.01 g · cm<sup>3</sup> = 1010 kg · m<sup>3</sup> for Zarrouk (FM) and  $\rho_m$  = 1.03 g · cm<sup>3</sup> = 1030 kg · m<sup>3</sup> for ASN-III (MM), the viscosity of Zarrouk ( $\mu$ ) = 7.49 × 10<sup>-4</sup> kg · m<sup>-1</sup>s<sup>-1</sup> and the viscosity of ASN-III ( $\mu$ ) = 9.11 × 10<sup>-4</sup> kg · m<sup>-1</sup>s<sup>-1</sup>, and the acceleration due to gravity ( $g$ ) = 9.8 m<sup>2</sup> · s.

**Table S11.** Average Stokes' velocity of NPI aggregates in ASN-III and Zarrouk.

NPI Concentrations	ASN-III		Zarrouk	
	Stokes' Velocity (mm · day <sup>-1</sup> )	Settling Distance after 48 Days (mm)	Stokes' Velocity (mm · day <sup>-1</sup> )	Settling Distance after 12 Days (mm)
2 mg L <sup>-1</sup> NPIs	7.0	333.6	1.7	20.0
10 mg L <sup>-1</sup> NPIs	4.4	210.5	1.8	21.3
20 mg/ L <sup>-1</sup> NPIs	2.7	131.2	1.6	19.6

### 1.10. Statistical Outputs

**Table S12.** The statistical outputs of the overall one-way analysis of variance (ANOVA) on PCC8806 and *Spirulina* growth rates, zeta potential (ZP) of cyanobacterial cells, and EPS concentrations in the presence of PS NPIs (2, 10, and 20 mg L<sup>-1</sup> NPIs); significant *p* values (*p* < 0.05) are displayed in bold text. *df* – degrees of freedom and F values are displayed.

<i>Strain</i>	<i>Parameter</i>	<i>Total df</i>	<i>F value</i>	<i>p-value</i>
<b>PCC8806</b>	Growth Rates	11	1.7952	0.2259
	ZP – pH 4	59	84.0424	< <b>0.0001</b>
	ZP – pH 5	59	25.7212	< <b>0.0001</b>
	ZP – pH 6	59	366.6037	< <b>0.0001</b>
	ZP – pH 7	59	206.1858	< <b>0.0001</b>
	ZP – pH 8	59	180.8379	< <b>0.0001</b>
	ZP – pH 9	59	162.1354	< <b>0.0001</b>
	ZP – pH 10	59	132.9779	< <b>0.0001</b>
	EPS Concentration	35	5.5031	<b>0.0037</b>
<i>Spirulina</i>	Growth Rates	11	1.7539	0.2334
	ZP – pH 4	59	7.8469	<b>0.0002</b>
	ZP – pH 5	59	39.5902	< <b>0.0001</b>
	ZP – pH 6	59	40.7148	< <b>0.0001</b>
	ZP – pH 7	59	1.8779	0.1438
	ZP – pH 8	59	2.6268	0.0592
	ZP – pH 9	59	1.7040	0.1766
	ZP – pH 10	59	2.2462	0.0929
	EPS Concentration	35	43.2814	< <b>0.0001</b>

**Table S13.** The statistical outputs of the overall one-way analysis of variance (ANOVA) on zeta potential and hydrodynamic diameter of PS NPIs in 0.1 M NaNO<sub>3</sub>; significant *p* values (*p* < 0.05) are displayed in bold text. *df* – degrees of freedom and F values are displayed.

<i>Zeta Potential</i>	<i>Total df</i>	<i>F value</i>	<i>p-value</i>
pH 4	26	11.9406	<b>0.0003</b>
pH 5	26	4.4528	<b>0.0227</b>
pH 6	26	35.2049	< <b>0.0001</b>
pH 7	26	40.9619	< <b>0.0001</b>
pH 8	26	49.6618	< <b>0.0001</b>
pH 9	26	41.3219	< <b>0.0001</b>
pH 10	26	57.6533	< <b>0.0001</b>
<i>Hydrodynamic Diameter</i>	<i>Total df</i>	<i>F value</i>	<i>p-value</i>
pH 4	26	492.5740	< <b>0.0001</b>
pH 5	26	416.1877	< <b>0.0001</b>
pH 6	26	25.4597	< <b>0.0001</b>
pH 7	26	13.7522	< <b>0.0001</b>
pH 8	26	1.5398	0.2349
pH 9	26	10.6984	< <b>0.0001</b>
pH 10	26	3.8580	<b>0.0352</b>

## 2. References

1. A. Liang, C. Paulo, Y. Zhu and M. Dittrich, CaCO<sub>3</sub> biomineralization on cyanobacterial surfaces: Insights from experiments with three *Synechococcus* strains, *Colloids and Surfaces B: Biointerfaces*, 2013, **111**, 600-608.
2. B. Raoof, B. D. Kaushik and R. Prasanna, Formulation of a low-cost medium for mass production of *Spirulina*, *Biomass and Bioenergy*, 2006, **30**, 537-542.
3. G. Hedenskog and A. V. Hofsten, The Ultrastructure of *Spirulina platensis* - A New Source of Microbial Protein, *Physiologia Plantarum*, 1970, **23**, 209-216.
4. M. Dittrich and S. Sibler, Influence of H<sup>+</sup> and Calcium Ions on Surface Functional Groups of *Synechococcus* PCC 7942 Cells, *Langmuir*, 2006, **22**, 5435-5442.

5. M. Tavafoghi, S. Garg, Korenevski. A. and M. Dittrich, Environmentally friendly antibiofilm strategy based on cationized phytyglycogen nanoparticles, *Colloids and Surfaces B: Biointerfaces*, 2021, **207**.
6. E. Kavitha, L. Devaraj Stephen, B. Fatema Hossain and S. Karthikeyan, Two-trace two-dimensional (2T2D) correlation infrared spectral analysis of *Spirulina platensis* and its commercial food products coupled with chemometric analysis, *Journal of Molecular Structure* 2021, **1244**, 130964.
7. C. Paulo, J. Kenney, P. Persson and M. Dittrich, Effects of Phosphorus in Growth Media on Biomineralization and Cell Surface Properties of Marine Cyanobacteria *Synechococcus*, *Geosciences*, 2018, **8**, 471.
8. A. Gélabert, O. S. Pokrovsky, J. Schott, A. Boudou, A. Feurtet-Mazel, J. Mielczarski, E. Mielczarski, N. Mesmer-Dudons and O. Spalla, Study of diatoms/aqueous solution interface. I. Acid-base equilibria and spectroscopic observation of freshwater and marine species, *Geochimica et Cosmochimica Acta*, 2004, **68**, 4039-4058.
9. J. J. Ojeda, M. E. Romero-González, R. T. Bachmann, R. G. J. Edyvean and S. A. Banwart, Characterization of the Cell Surface and Cell Wall Chemistry of Drinking Water Bacteria by Combining XPS, FTIR Spectroscopy, Modeling, and Potentiometric Titrations, *Langmuir*, 2008, **24**, 4032-4040.
10. Y. Dong, M. Gao, Z. Song and W. Qiu, As(III) adsorption onto different-sized polystyrene microplastic particles and its mechanism, *Chemosphere*, 2020, **239**, 124792.